The Canadian Mineralogist
Vol. 39, pp. 1529-1546 (2001)

BORON DEPLETION CONTROLLED BY THE BREAKDOWN OF TOURMALINE IN THE MIGMATITE ZONE OF THE AOYAMA AREA, RYOKE METAMORPHIC BELT, SOUTHWESTERN JAPAN

TETSUO KAWAKAMI

Department of Geology and Mineralogy, Graduate School of Science, Kyoto University, Kyoto 606-8502, Japan

Abstract

A drastic drop of whole-rock boron contents is observed across the tourmaline-out isograd located near the schist–migmatite boundary of the Aoyama area, Ryoke metamorphic belt, southwestern Japan. The variation in whole-rock boron contents corresponds well with the modal proportion of tourmaline; most of the boron is contained in tourmaline in the upper-amphibolite-facies metasedimentary rocks. The drastic drop in whole-rock boron contents, from 10–79 to <5 ppm across the tourmaline-out isograd, may be caused by the breakdown of tourmaline accompanied by the extraction of a small amount of boron-bearing melts or fluids from the migmatite zone. Tourmaline-bearing pegmatite veins observed to the north of the tourmaline-out isograd are one of the important sinks of boron considered to have been extracted from the migmatite zone. The behavior of boron in muscovite and tourmaline is modeled on the P–T path of the Aoyama area. Near the P–T conditions of its breakdown, the $^{X}\square AlNa_{-1}Mg_{-1}$ exchange is insignificant in tourmaline, whereas the $Al_2Mg_{-1}Si_{-1}$, $AlOMg_{-1}(OH)_{-1}$ and $CaMg_2{}^{X}\square_{-1}{}^{Y}Al_{-2}$ or $CaMgO^{X}\square_{-1}{}^{Y}Al_{-1}(OH)_{-1}$ exchanges are important. The amount of the *X*-site vacancy is controlled by the incorporation of Ca into tourmaline.

Keywords: boron, tourmaline, partial melting, migmatite, muscovite, P–T path, high-grade metamorphism, crystal chemistry, Ryoke metamorphic belt, Japan.

Sommaire

La teneur globale en bore diminue de façon abrupte en traversant l'isograde marquant la disparition de la tourmaline près de l'interface entre schistes et migmatites dans la région de Aoyama, ceinture métamorphique de Ryoke, dans le secteur sud-ouest du Japon. La variation en bore correspond bien à la proportion de tourmaline dans ces roches métasédimentaires; la plupart du bore loge dans la tourmaline dans ces roches équilibrées au faciès amphibolite supérieur. La chute abrupte de la teneur en bore, de 10–79 à <5 ppm en traversant l'isograde, pourrait s'expliquer par la déstabilisation de la tourmaline, et l'extraction de faibles volumes de liquite silicaté ou phase fluide borifère provenant de la zone de migmatites. Des veines pegmatitiques à tourmaline, observées au nord de l'isograde, seraient un des réservoirs importants pour le bore extrait de la zone des migmatites. Le comportement du bore dans la muscovite et la tourmaline est analysé dans le contexte local de la région de Aoyama et de son évolution P–T. Près des conditions de sa déstabilisation, le couple de substitution $^{X}\square AlNa_{-1}Mg_{-1}$ n'est pas important dans la tourmaline; en revanche, les vecteurs d'échange $Al_2Mg_{-1}Si_{-1}$, $AlOMg_{-1}(OH)_{-1}$ et $CaMg_2{}^{X}\square_{-1}{}^{Y}Al_{-2}$ ou $CaMgO^{X}\square_{-1}{}^{Y}Al_{-1}(OH)_{-1}$ sont importants. La proportion de lacunes dans le site *X* serait régi par la teneur en Ca de la tourmaline.

(Traduit par la Rédaction)

Mots-clés: bore, tourmaline, fusion partielle, migmatite, muscovite, tracé P–T, degré de métamorphisme élevé, chimie cristalline, ceinture métamorphique de Ryoke, Japon.

E-mail address: kawakami@kueps.kyoto-u.ac.jp

Introduction

Differentiation of crustal material through partial melting is a very important process in the chemical evolution of the continental crust. Migmatite zones in high-grade parts of the regional metamorphic belts have been considered by many investigators to represent sites where such chemical differentiation may have taken place (*e.g.*, Brown *et al*. 1995, Brown & Rushmer 1997, Sawyer 1996, Williams *et al*. 1995).

Tourmaline was found to be absent in the migmatite zone, and the tourmaline-out isograd is clearly defined in the upper amphibolite-facies anatectic migmatite zone of the Aoyama area, Ryoke metamorphic belt, southwestern Japan (Kawakami 2000, 2001). Tourmaline is the most important boron-bearing mineral in high-grade pelitic–psammitic metamorphic rocks. Therefore, the stability of tourmaline may control the behavior of whole-rock boron. It is known that terrestrial sediments normally contain about 100 ppm boron (London *et al.* 1996), typically incorporated in illite and muscovite in low-grade metasediments. Up to the lower amphibolite facies, boron released through dehydration reactions of these minerals is considered to contribute to the formation of an overgrowth on tourmaline (Henry & Dutrow 1990a), which becomes an important sink of boron (Sperlich *et al.* 1996) in the upper-amphibolite-facies metasediments. However, this fact has not been shown from petrological data. In this paper, I show that tourmaline is the most important sink of boron in the Aoyama area.

At high metamorphic grades, other borosilicates such as grandidierite and kornerupine are known to occur in some granulites; such borosilicates and sillimanite become important sinks of boron (*e.g.*, Grew & Hinthorne 1983). However, granulites and migmatites with such minerals are rare, and they are typically depleted in boron (Shaw *et al*. 1988, Leeman *et al*. 1992, Moran *et al*. 1992, Bebout *et al*. 1993). Depletion of boron in granulites and migmatites has been ascribed to subsolidus dehydration-type reactions involving illite and muscovite, among others, and concomitant extraction of boron-bearing fluids during prograde metamorphism (*e.g.*, Leeman *et al*. 1992, Moran *et al*. 1992, Bebout *et al*. 1993).

The breakdown of tourmaline releases boron to the surroundings if other boron-bearing minerals are not formed. Boron lowers the solidus temperature of the rocks (Pichavant 1981) and the viscosity of melts (Dingwell *et al.* 1992). These effects may promote a more effective segregation of melt. In this way, the behavior of boron is especially important in anatectic zones (Pereira & Shaw 1997, Acosta *et al*. 2000, 2001). Boron also is important because it behaves as an incompatible element in the absence of stable borosilicates. A study of the field distribution of boron and borosilicates can, therefore, shed light on the movement of melt or fluid (or supercritical fluid) during metamorphism.

The tourmaline-out isograd in the Aoyama area (Kawakami 2001) provides a good example of the effect of tourmaline breakdown and extraction of melts or fluids on the depletion of whole-rock boron contents. In the present study, a drastic decrease of whole-rock boron contents across the tourmaline-out isograd was confirmed for the first time; the mechanism for the decrease of boron in the migmatite zone is discussed from the viewpoint of the P–T evolution of the rocks.

In spite of the importance of tourmaline breakdown phenomena, the chemical composition and crystal chemistry of tourmaline at the P–T conditions in which tourmaline breaks down have not been reported in detail from field evidence. There have been many experimental studies on the tourmaline breakdown (*e.g.*, Benard *et al*. 1985, Morgan & London 1989, Holtz & Johannes 1991, Schreyer & Werding 1997, von Goerne *et al*. 1999, 2001, von Goerne & Frantz 2000) and data from the field study have been required (*e.g.*, von Goerne *et al*. 1999). In this paper, a detailed description of the composition of tourmaline is reported for the first time from a field area, and is compared with the results of the experimental studies.

Geological Setting of the Ryoke Metamorphic Belt and Petrography

The Ryoke metamorphic belt extends for approximately 800 km in length, and has a width of 30–50 km (Fig. 1). It is accompanied by abundant granites, and metamorphic rocks occupy only 20–30% of the belt. The Ryoke metamorphic belt offers one of the best-known examples of the low-P/T type metamorphism (*e.g.*, Miyashiro 1965, 1994, Brown 1998, Ikeda 1993, 1998a, b, Okudaira *et al*. 1993, Okudaira 1996, Nakajima *et al*. 1990, Nakajima 1994, Suzuki & Adachi 1998). The intermediate- to high-P/T type Sanbagawa belt is located to the south of the Ryoke metamorphic belt. The two belts are separated by the Median Tectonic Line (MTL).

The protoliths of the Ryoke metamorphic rocks are the Jurassic accretionary Mino–Tanba belt exposed to the north of the Ryoke belt (Wakita 1987). Metamorphic grade generally increases toward the south. The highest-grade metamorphic rocks are characterized by the coexistence of garnet and cordierite in pelitic–psammitic rocks (*e.g.*, Ono 1977, Ikeda 1998b); the peak pressure–temperature conditions are estimated to have been up to *ca.* 5 kbar and *ca.* 850ºC (Brown 1998).

Migmatites are developed in the high-grade parts of the Ryoke metamorphic belt, such as in the cordierite – K-feldspar, sillimanite – K-feldspar and garnet–cordierite zones of the Yanai district (Higashimoto *et al.* 1983, Ikeda 1998b, Brown 1998) and the K-feldspar–cordierite and garnet–cordierite zones of the Takato–Kashio district (Brown 1998).

There are two types of granite in the Ryoke belt, gneissic granite (Older Ryoke granite) and massive granite (Younger Ryoke granite). Generally, the massive

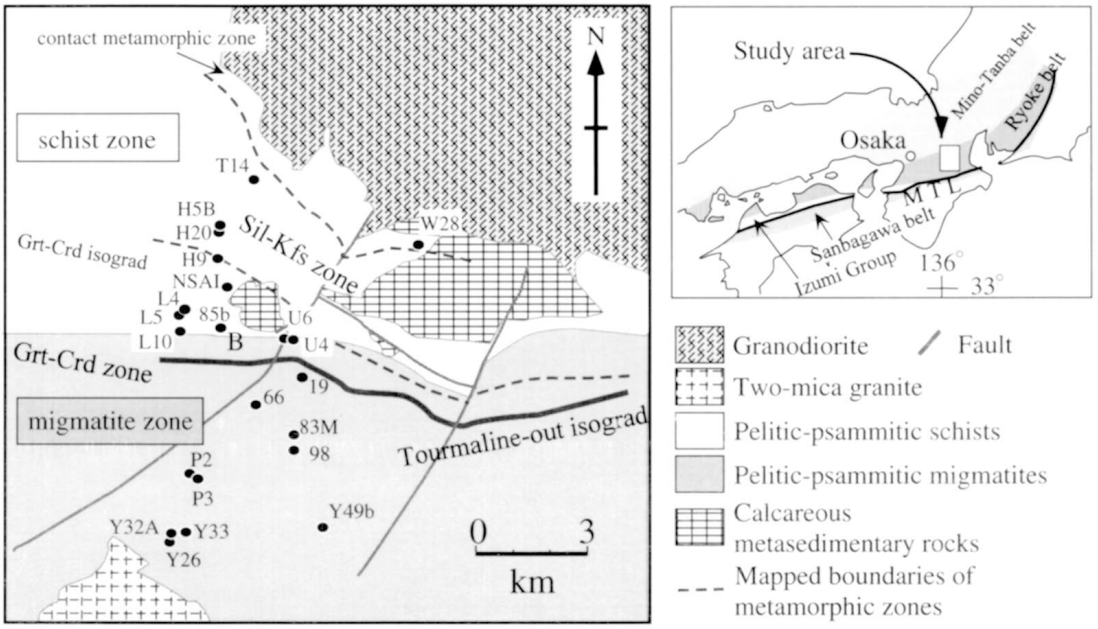

FIG. 1. A simplified geological map of the Aoyama area. The tourmaline-out isograd is also shown. It is subparallel to the garnet–cordierite isograd formed through regional metamorphism. Locations of samples used in this study are shown as black dots. The location of boudin necks filled with leucosome is shown by 'B'. Tourmaline-bearing pegmatite veins are found at the locality NSAI. Modified from Kawakami (2001).

granites postdate the gneissic granites in the Ryoke belt. Although granites are abundant, the regional metamorphic isograds are generally independent of the outline of massive granitic plutons that cross-cut the metamorphic rocks (Higashimoto *et al*. 1983). Gneissic granites are considered to be the heat source for the Ryoke metamorphism (*e.g.*, Okudaira 1996, Ikeda 1998b); they occur concordantly with the schistosity of high-grade metamorphic rocks, and are not associated with a contact aureole (*e.g.*, Okudaira *et al*. 1993).

The CHIME (chemical Th – U – total Pb isochron method) dating of monazite from pelitic–psammitic migmatites gives ages between 102 and 98 Ma both in the eastern and western parts of the belt. These ages presumably represent the time of the first attainment of *ca*. 525ºC during the Ryoke metamorphism, and the peak metamorphism was contemporaneous with the intrusion of the oldest Older Ryoke granite plutons, *ca*. 95 Ma (Suzuki & Adachi 1998).

The Aoyama area

The Aoyama area is located about 25 km north of the MTL and 80 km east of Osaka (Fig. 1). High-grade metamorphic rocks are widely distributed in this area (Yoshizawa *et al*. 1966, Hayama *et al*. 1982, Takahashi & Nishioka 1994, Kawakami 2001). The main rock types are metapelite and metapsammite with subordinate amounts of metachert, metabasite and calcareous metasediments. The pelitic–psammitic rocks are schists in the north, and are metatexite to inhomogeneous diatexite (Brown 1973) in the south. Foliation of the metamorphic rocks trends east–west and dips moderately to the north.

In the Aoyama area, three metamorphic zones are exposed: the contact-metamorphic zone, the sillimanite – K-feldspar zone and the garnet–cordierite zone. All three zones are above the second sillimanite isograd (Hayama *et al*. 1982). The grade of regional metamorphism increases from north to south. The peak pressure–temperature conditions are 620–650°C, 3.0–4.0 kbar for the sillimanite – K-feldspar zone, and 650–800°C, 4.0–6.0 kbar for the garnet–cordierite zone. The pressure estimates suggest that deeper structural levels of the metamorphic belt are exposed to the south of the Aoyama area (Kawakami 2001).

In addition to the metamorphic rocks, massive granodiorite occurs at the northern edge of the Aoyama area. The granodiorite pluton is discordant with respect to the schistosity of the metamorphic rocks and is associated with a contact-metamorphic aureole (Takahashi & Nishioka 1994, Kawakami 2001). The granodiorite pluton contains xenoliths of the Ryoke metamorphic rocks (Yoshida *et al*. 1995), suggesting that the intru-

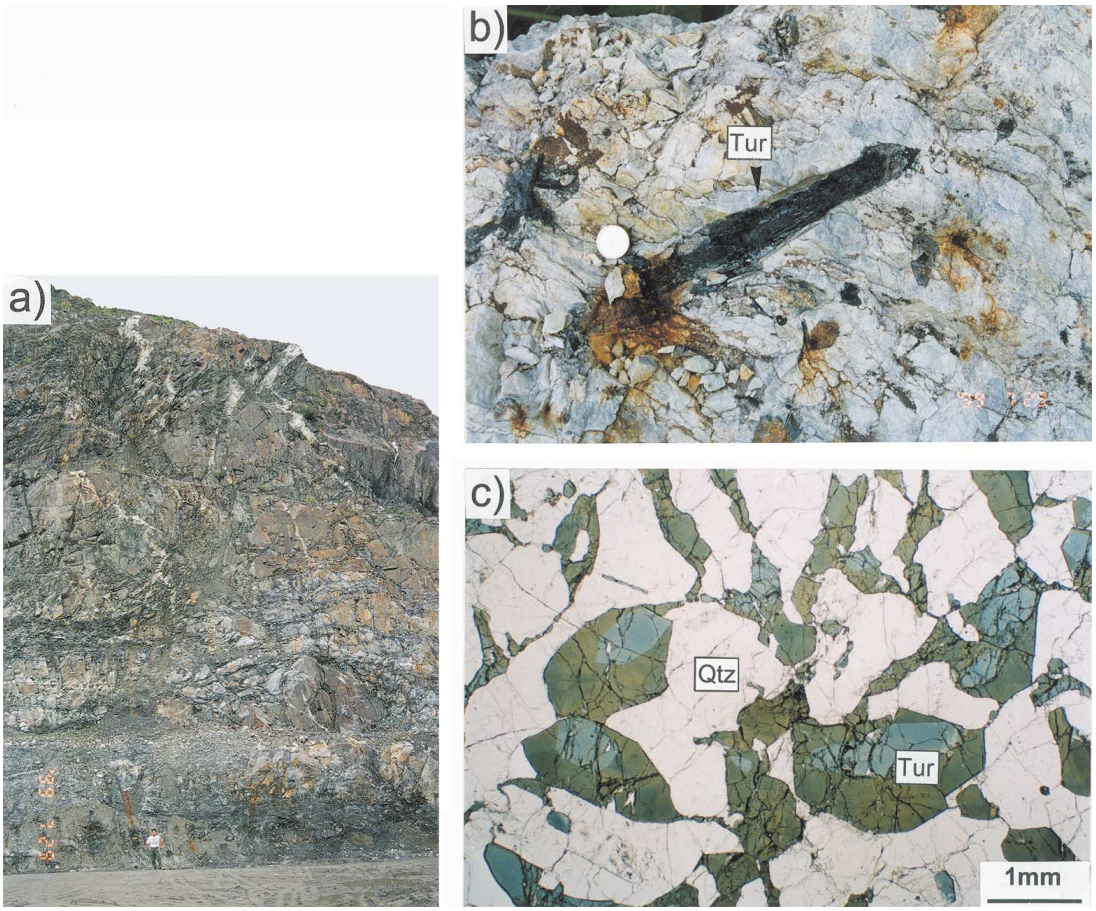

FIG. 2. Photographs and photomicrographs showing the mode of occurrence of tourmaline in the pegmatite veins to the north of the tourmaline-out isograd (Locality NSAI, Fig. 1). a) Tourmaline-bearing pegmatite veins (white veins) to the north of the isograd. Veins are intruded almost vertically and perpendicular to the schistosity of the pelitic–psammitic rocks. b) A euhedral crystal of tourmaline in the pegmatite vein. The diameter of the coin is 2 cm. c) Tourmaline–quartz intergrowth observed in the pegmatite sample. The tourmaline has a weak chemical zoning. Plane-polarized light.

sion of the granodiorite postdates the formation of the Ryoke metamorphic rocks.

Another pluton of massive two-mica granite occurs at the southern margin of the metamorphic rocks and cross-cuts the schistosity of the metamorphic rocks. This pluton belongs to the Younger Ryoke granites, and there is no evidence for contact metamorphism.

Veins of tourmaline-bearing granitic pegmatite occur to the north of the tourmaline-out isograd (locality NSAI in Fig. 1). They are exposed in a quarry several hundred meters wide (Fig. 2a). Pegmatite veins cross-cut the schistosity of the pelitic–psammitic schists nearly vertically. One pegmatite vein is found in each 10 m of exposure on average, and at least five large veins are observed within the quarry. The veins are at most about one meter in width and become thinner at the deeper structural levels. Tourmaline of schorl-rich composition (Table 1) is present in the veins, and the largest crystal of tourmaline observed is 3.5 cm in diameter and 25 cm in length (Fig. 2b). Ten tourmaline crystals were found within 1 m^2. Other constituent minerals are quartz (crystals up to 40 cm in diameter), plagioclase, K-feldspar and minor amounts of biotite and garnet. Although garnet is rare, it coexists with tourmaline. A minor amount of biotite also is found with tourmaline. Tourmaline also forms a tourmaline–quartz intergrowth, as shown in Figure 2c. Veins of biotite-bearing pegmatite devoid of tourmaline crystals also occur at the same locality.

TABLE 1. COMPOSITION OF TOURMALINE FROM A TOURMALINE–QUARTZ INTERGROWTH IN A PEGMATITE VEIN, AOYAMA AREA, JAPAN

sample	99N1 N0203 gr-yel rim	99N1 N0104 gr-yel rim	99N1 N0103 pale gr mantle	99N1 N0101 pale gr core	99N1 N0102 gr-yel core
B_2O_3 wt% *	10.30	10.31	10.40	10.33	10.23
SiO_2	35.77	35.67	36.52	36.12	35.62
TiO_2	0.35	0.38	0.11	b.d.	0.25
Al_2O_3	33.24	33.57	33.99	33.41	32.25
FeO	10.31	10.48	10.34	10.13	10.34
MnO	0.24	0.20	0.18	0.20	0.20
MgO	3.23	3.04	2.86	3.33	3.80
CaO	0.28	0.28	0.14	0.27	0.26
Na_2O	1.85	1.72	1.79	1.87	1.90
Total	95.57	95.65	96.33	95.66	94.85
B *apfu* *	3.00	3.00	3.00	3.00	3.00
Si	6.04	6.01	6.10	6.08	6.05
Ti	0.04	0.05	0.01	-	0.03
Al	6.61	6.67	6.70	6.63	6.46
Fe	1.46	1.48	1.45	1.43	1.47
Mn	0.03	0.03	0.03	0.03	0.03
Mg	0.81	0.76	0.71	0.83	0.96
Ca	0.05	0.05	0.03	0.05	0.05
Na	0.61	0.56	0.58	0.61	0.63
Mg/[Mg + Fe(tot)]	0.36	0.34	0.33	0.37	0.40

b.d.: below detection limit. * Calculated for 3 boron cations per formula unit. K: below detection limit in all cases. gr-yel: green-yellow. *apfu*: atoms per formula unit. The tourmaline from pegmatite veins are richer in the schorl component that the tourmaline in the matrix (*cf.* Kawakami 2001).

The Tourmaline-Out Isograd and Description of Tourmaline in the Pelitic–Psammitic Metamorphic Rocks

Details of the mode of occurrence of tourmaline in the pelitic–psammitic metamorphic rocks (Kawakami 2001) are briefly summarized below. Chemical change observed in the tourmaline from north of the tourmaline-out isograd are documented in detail because this study is among the first to report the compositional change of tourmaline at the P–T conditions of tourmaline breakdown in a field setting.

The distribution of tourmaline is restricted to the northern half of the Aoyama area, whereas it is entirely absent in the southern half. The tourmaline-out isograd is located near the schist–migmatite transition boundary and is subparallel to the garnet–cordierite isograd formed during regional metamorphism. Grains of tourmaline are progressively surrounded by an intergrowth of sillimanite and cordierite (see Figs. 6e and 7 of Kawakami 2001) near the tourmaline-out isograd (locality B in Fig. 1). This reaction texture is found in the pelitic–psammitic sample accompanied with boudin necks filled with tourmaline-bearing leucosome. The leucosome at the boudin necks consists of quartz, plagioclase (locally idiomorphic), K-feldspar, tourmaline, and subordinate amount of muscovite, andalusite, cordierite, biotite and apatite. The former presence of tourmaline throughout the study area is suggested by the rare occurrence of irregularly shaped tourmaline and tourmaline inclusions in other minerals to the south of the isograd. From these observations, the dehydration-melting reaction that may account for the tourmaline-out isograd is inferred to be (Kawakami 2001)

$$\text{Tur} + \text{Bt} + \text{Kfs} + \text{Ab} + \text{Qtz} = \text{Sil} + \text{Crd} + \text{melt}. \quad (1)$$

Two types of tourmaline are recognized in the pelitic–psammitic schists to the north of the tourmaline-out isograd. An inclusion-poor type consists of crystals of schorl–dravite series aligned parallel to the schistosity. It shows weak compositional zoning, and the tourmaline with the reaction texture mentioned above is limited to this type. An inclusion-rich type of tourmaline occurs with bundles of sillimanite ("fibrolite") that cross-cut the main schistosity, suggesting its retrograde origin. This type does not occur near the tourmaline-out isograd, and thus does not seem to be directly related to the breakdown of tourmaline during prograde metamorphism.

The chemical composition of tourmaline was determined using a scanning electron microscope (Hitachi S550) with an energy-dispersion X-ray analytical system (Kevex 8000 + Kevex Quantum detector) at Kyoto University. The analytical procedure follows that of Mori & Kanehira (1984) and Hirajima & Banno (1991). On the basis of counting statistics, an analytical precision 1σ is estimated to be better than 0.25% for Si, 4.0% for Ti (15% for tourmaline in pegmatite veins), 0.3% for Al, 6% for Ca (15% for samples containing less than 0.2 wt% CaO), 0.65% for Fe (1.0% for inclusion-rich type tourmaline), 1.2% for Mg (2.1% for tourmaline in pegmatite veins), 7.2% for Mn in tourmaline in pegmatite veins, and 3.6% for Na, respectively.

The formulae of tourmaline from pelitic–psammitic rocks were normalized on the basis of 15 cations exclusive of B, Na, K and Ca. This approach assumes no vacancies in the tetrahedral and octahedral sites and insignificant Li content (Henry & Dutrow 1996). The amount of B was calculated from stoichiometric constraints (*e.g.*, Henry & Guidotti 1985, Hawthorne 1996, Dutrow *et al.* 1999), with the assumption that ^{IV}B is absent. The formula of tourmaline and the name of the sites used in this paper follow the recommendations of Hawthorne & Henry (1999); $XY_3Z_6[T_6O_{18}][BO_3]_3V_3W$.

Analyzed samples are W28 (contact-metamorphic zone), H5B, H20 (sillimanite – K-feldspar zone), L5, L10, U6 (low-temperature part of the garnet–cordierite zone), SAI991 (a sample containing tourmaline with breakdown texture and tourmaline in the boudin neck filled with leucosome; locality B), and 99N1N (pegmatite; locality NSAI). The results of the analyses are shown in Figure 3.

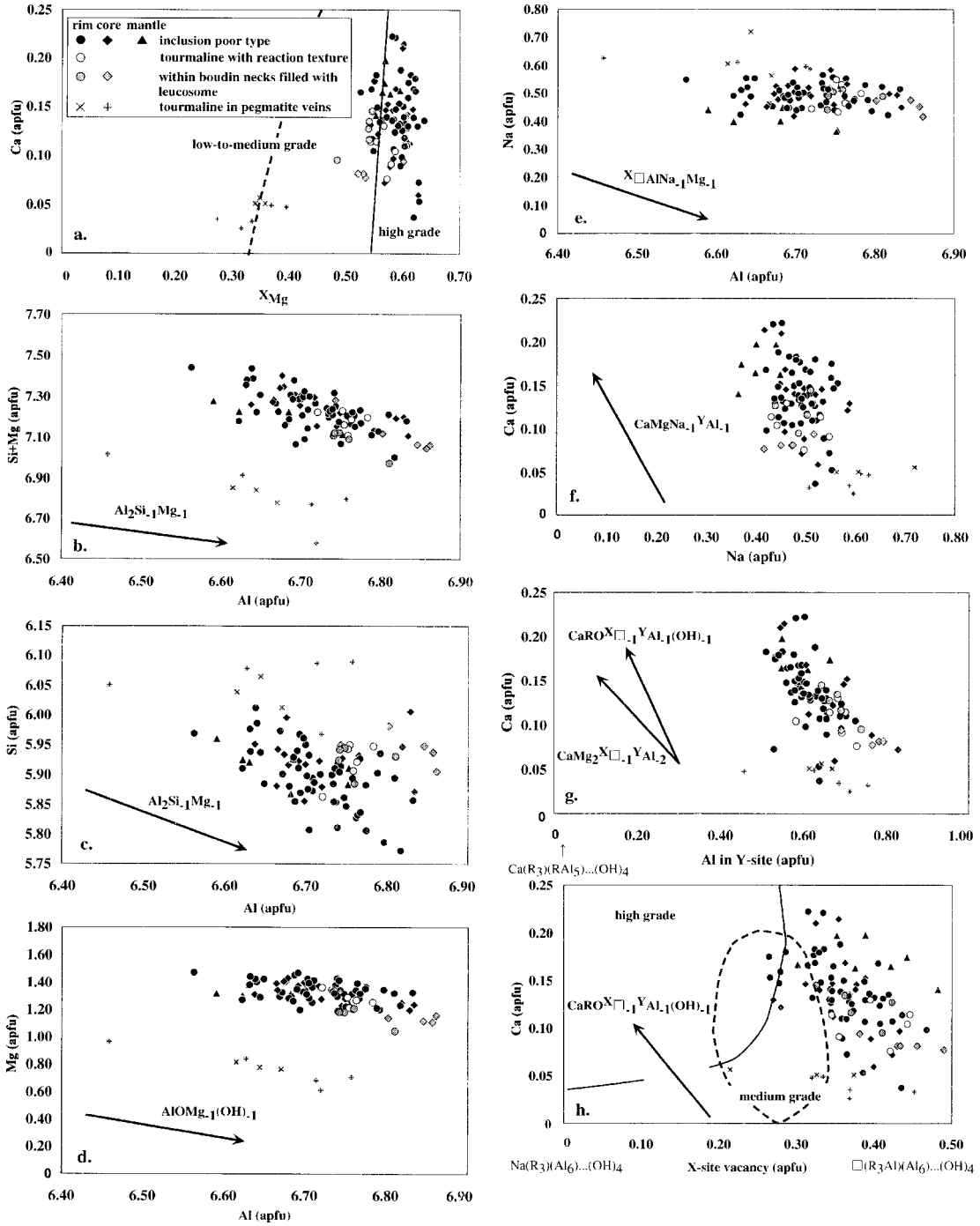

FIG. 3. Compositional relations between the inclusion-poor type of tourmaline, tourmaline with a reaction texture, tourmaline contained in the boudin necks filled with leucosome, and tourmaline in pegmatite veins. The fields of "low-to-medium grade" or "medium grade" (dashed line) and "high grade" (solid line) metasedimentary rocks of Henry & Dutrow (1996) are shown for comparison. See text for details.

TABLE 2. MAJOR-ELEMENT COMPOSITION, BORON CONTENT, MINERAL ASSEMBLAGE, AOYAMA AREA, JAPAN

	SiO_2	TiO_2	Al_2O_3	Fe_2O_3	MnO	MgO	CaO	Na_2O	K_2O	P_2O_5	total	B	Tur*	B§	Rock type	And	Sil	Grt	Crd	Bt	Ms	Tur
MINO	70.11	0.80	16.56	5.12	0.02	1.55	0.18	1.84	3.68	0.16	100.0	112			pelitic schist							
T14	59.87	0.89	18.20	5.39	0.04	2.56	1.64	2.25	7.90	0.17	98.9	3	0.00	0	pelitic schist	-	-	-	-	+	-	-
W28	68.49	0.66	15.76	5.45	0.14	2.08	1.70	1.96	3.53	0.18	100.0	64	0.24	84	pelitic-psammitic schist	-	-	+	-	+	+	+
H20	68.55	0.85	15.33	7.03	0.11	2.65	0.28	0.61	4.33	0.10	99.8	79	0.18	63	pelitic schist	-	+	-	-	+	+	+
H9	54.24	1.21	18.59	9.81	0.14	2.04	1.84	2.81	8.29	0.45	99.4	31	0.08	33	pelitic schist	-	-	-	-	+	-	+
NSAI	63.65	0.77	17.89	6.00	0.10	2.23	2.40	3.15	3.64	0.20	100.0	17	0.02	4	pelitic-psammitic schist	-	-	-	-	+	+	+
L5	64.49	0.80	18.33	5.82	0.08	2.17	1.47	2.41	4.09	0.21	99.9	77	0.23	78	pelitic schist	+	+	-	-	+	+	+
85b	65.04	0.76	17.75	5.72	0.13	2.02	2.06	2.83	3.52	0.18	100.0	2	0.00	0	psammitic schist	-	-	-	-	+	-	-
L10	66.25	0.74	17.73	5.45	0.11	1.84	1.51	2.55	3.55	0.14	99.9	19	0.04	11	pelitic schist	+	+	-	-	+	+	+
U6	69.03	0.65	15.83	4.49	0.05	1.73	2.23	3.68	2.31	0.20	100.2	10	0.02	4	metatexite	-	-	-	-	+	+	+
U4	69.26	0.59	16.09	5.23	0.22	1.59	1.41	3.13	2.50	0.10	100.1	< 2			metatexite	-	+	-	+	+	+	-
19	65.18	0.89	16.40	6.44	0.08	2.33	1.92	3.29	3.13	0.18	99.8	< 2			metatexite	-	-	+	-	+	+	-
66	66.04	0.72	17.34	5.22	0.11	2.02	1.77	2.65	4.02	0.17	100.1	2			metatexite	-	+	+	+	+	+	-
83M	61.73	0.88	17.99	7.09	0.19	2.39	2.19	4.06	3.09	0.12	99.7	< 2			metatexite	-	+	+	+	+	+	-
98	66.94	0.58	16.56	5.04	0.19	1.84	2.53	4.33	2.03	0.11	100.2	< 2			psammitic metatexite	-	-	+	-	+	+	-
P2	63.34	1.01	17.15	6.76	0.07	2.35	2.49	3.66	2.70	0.11	99.6	< 2			heterogeneous diatexite	-	+	+	+	+	+	-
P3	69.13	0.55	15.96	3.50	0.05	1.12	1.36	2.87	5.30	0.30	100.1	3			heterogeneous diatexite	-	+	-	+	+	+	-
Y33	70.14	0.59	16.43	3.99	0.04	1.62	1.47	2.44	3.23	0.10	100.0	5			heterogeneous diatexite	-	+	-	+	+	+	-
Y32A	63.81	0.96	17.79	7.24	0.09	2.43	1.53	2.54	3.63	0.10	100.1	4			metatexite	-	+	-	+	+	+	-
Y26	60.80	1.19	19.26	8.32	0.09	3.22	0.94	1.54	4.19	0.08	99.6	< 2			melanosome-rich metatexite	-	+	+	+	+	+	-
SAI991B	74.98	0.14	14.72	0.93	0.02	0.42	0.66	1.57	5.75	0.24	99.4	745			Tur-bearing leucosome							
SAIT1B	73.96	0.08	15.12	0.47	0.01	0.18	0.64	1.77	7.12	0.21	99.6	283			Tur-bearing leucosome							
SAIT2B	75.10	0.09	14.29	0.56	0.01	0.25	0.51	1.58	6.89	0.18	99.5	273			Tur-bearing leucosome							

The bulk compositions were determined by X-ray fluorescence analysis, and the boron content, by prompt gamma atomic aborption analysis (PGNAA). The detection limit for boron by this technique is 2 ppm; <2 ppm indicates that the amount of boron is below the detection limit. Symbols of minerals follow Kretz (1983). Muscovite is a product of retrograde metamorphism. Where present, andalusite is partly transformed into sillimanite. Major-element oxides in wt%, boron in ppm. +: present, -: absent. Sample MINO is from the Mino–Tamba belt. Sample H20 contains veins of "fibrolite". Sample L5 is andalusite-bearing. Samples SAI991B, SAIT1B and SAIT2B: tourmaline-bearing leucosome in boudin neck. * Tur mode, in vol.%. § Calculated.

On the basis of the classification of Hawthorne & Henry (1999), most of the tourmaline compositions in the Aoyama area belong to the alkali group. Several tourmaline compositions, such as the mantle compositions of tourmaline contained in sample H20, belongs to the *X*-site-vacant group. EDX analyses showed that F is absent or nearly absent. Assuming the *V* and *W* sites to be fully occupied with OH (*e.g.*, Henry & Dutrow 1996), almost all the tourmaline compositions fall in the field of dravite. The exceptions are tourmaline in the pegmatite veins, which fall in the field of schorl.

The core, mantle and rim parts of the inclusion-poor type of tourmaline show almost the same composition. They plot on the trend of several exchange-vectors (Fig. 3), which will be discussed in detail below. Tourmaline crystals in sample L5 show signs of sector zoning in the rim, suggesting a rapid growth of the rim part. Addition of the compositions of chemically sector-zoned tourmaline to Figure 3 makes no difference on the chemical trend shown in the figure. Tourmaline from the sillimanite – K-feldspar zone, the low-temperature part of the garnet – cordierite zone and the contact-metamorphic zone plots almost in the same region. Therefore, tourmaline from these three zones, including sample L5, are plotted together as the "inclusion-poor type" (Fig. 3).

Tourmaline in the leucosome that is filling the boudin necks has a slightly lower X_{Mg} than the matrix tourmaline and plots concordantly on the same chemical trend mentioned above. Tourmaline in the pegmatite veins has the lowest X_{Mg} of any tourmaline in the Aoyama area and plots away from other types of tourmaline.

The inclusion-rich type of tourmaline shows the highest X_{Mg} value (0.59–0.67 in the core, 0.60–0.78 in the mantle, and 0.64–0.69 in the rim) of any tourmaline in the Aoyama area. The core part of this type tends to be the poorest in Al (6.00–6.49 *apfu*, atoms per formula unit) among all the tourmaline types, whereas the rim part has almost the same Al value (6.63–6.76 *apfu*) as the inclusion-poor type of tourmaline. The variation of the *X*-site vacancy of this type is almost identical to that of the inclusion-poor type of tourmaline.

Determination of Whole-Rock Boron Contents and Modal Proportions of Tourmaline

The whole-rock boron contents were determined for 19 samples from the Aoyama area and one sample from

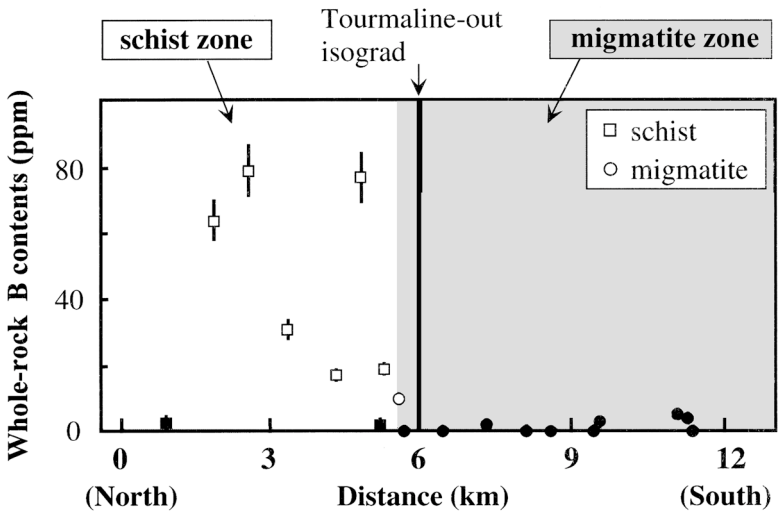

FIG. 4. The variation in whole-rock boron contents. Squares represent schist samples and circles represent migmatite samples. Solid symbols represent tourmaline-free samples, whereas open symbols represent the samples containing tourmaline. Error bars show ±5% error in the measured value of boron by PGNAA where the value exceeds 5 ppm (Shaw & Smith 1991, Pereira & Shaw 1997). At lower contents, ± double the amount of blank (±2 ppm) is shown as error bars for the measured value of boron. Note the drastic drop of whole-rock boron contents across the tourmaline-out isograd and the good correspondence of boron contents with presence or absence of tourmaline.

the Mino–Tanba belt by prompt gamma neutron-activation analysis (PGNAA) at Centre for NAA, McMaster University (Higgins *et al*. 1984). Nine samples of pelitic–psammitic schists (including one pelitic rock sample from the Mino–Tanba belt) and 11 samples of pelitic–psammitic migmatites were analyzed. Detailed information on each sample is given in Table 2.

A rock sample of *ca*. 500 cm^3 was cut perpendicular to the foliation or migmatite banding into several rock plates and then crushed into small fragments in a clean plastic bag. A 100-g sample was randomly selected and powdered in a tungsten carbide mill. Migmatite samples show leucosome–melanosome banding on a millimeter scale (up to 10 mm); leucosome and melanosome were crushed together. The powder sample was carefully prepared to prevent boron contamination.

Half a gram of the powdered sample was used for the PGNAA of boron; the detection limit is 2 ppm. The accuracy and precision have been assessed by Shaw & Smith (1991). The precision of the single analysis is generally better than ±5% where boron content exceeds 5 ppm. The results of the analyses are given in Table 2 and Figure 4.

Whole-rock boron contents of the schists from the north of the tourmaline-out isograd containing tourmaline vary from 17 to 79 ppm (shown with open squares in Fig. 4), whereas those without tourmaline show low boron contents (2–3 ppm; shown with solid squares).

On the other hand, pelitic–psammitic migmatites from south of the isograd are all free of tourmaline and show very low boron contents (<5 ppm; shown with solid circles). One migmatite sample taken from the vicinity of the tourmaline-out isograd (sample U6) exceptionally contains tourmaline crystals and shows slightly higher boron content (10 ppm; shown with an open circle) than the other tourmaline-free migmatite samples. From Figure 4, it is clear that samples containing tourmaline crystals generally show high boron contents, and a drastic decrease of whole-rock boron contents is observed across the tourmaline-out isograd.

The boron contents of the tourmaline-bearing leucosome that is filling the boudin necks were also determined for three samples (Table 2). In addition, the boron content of one pelitic sample from the Mino–Tanba belt is also reported (Table 2).

The powdered samples prepared for the PGNAA were heated for three hours in an electric furnace at 900°C in order to decompose the graphite present, and were utilized in the XRF analyses for major elements with Rigaku simultaneous X-ray spectrometer, system 3550. The analytical procedure follows that of Goto & Tatsumi (1994). The results are given in Table 2 and are plotted in Figure 5.

In the ACF, AKF and AFM plots of the whole-rock compositions (Fig. 5), several samples (samples H9, H20, P3 and T14) plot slightly outside the cluster of the

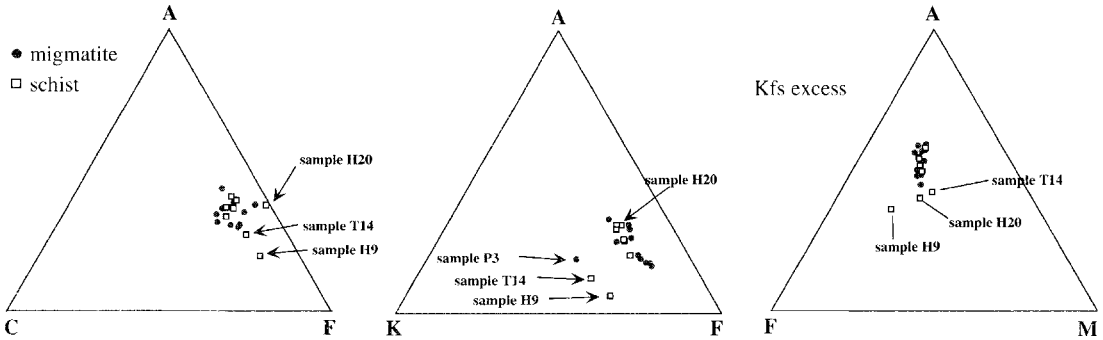

FIG. 5. ACF, AKF and AFM plots (projected from K-feldspar) of whole-rock compositions of pelitic–psammitic rocks in the Aoyama area. Open squares represent schist samples, and solid circles represent migmatite samples. Note that whole-rock compositions of pelitic–psammitic schists and migmatites plot in almost the same area.

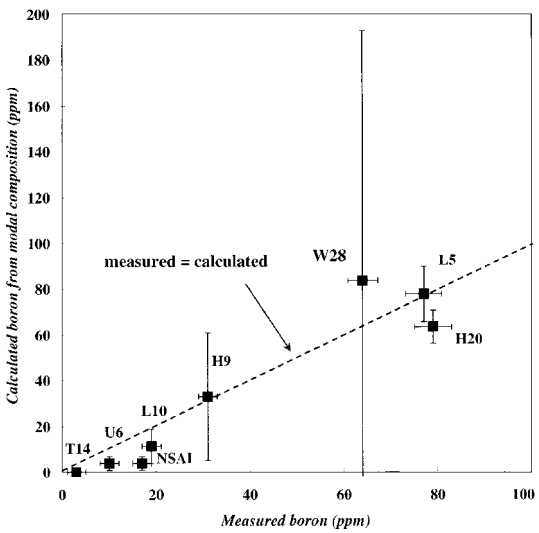

FIG. 6. Relationship between measured whole-rock boron contents in the pelitic–psammitic rocks and whole-rock boron contents calculated from the modal proportion of tourmaline. Error bars show 2σ error on the modal count, and the same as Figure 4 for measured value of boron. Dashed line represents the ideal 1:1 ratio for measured and calculated whole-rock boron contents. Good accordance between these two values implies that whole-rock boron is almost completely contained in tourmaline.

majority of the analyzed samples. In terms of major elements, however, the whole-rock compositions of the pelitic–psammitic schists and migmatites are almost the same (Fig. 5).

Modal proportions of tourmaline for samples from north of the tourmaline-out isograd have been determined under the microscope by point counting. Representative pieces of rock used in the whole-rock chemical analyses (XRF and PGNAA) were selected for preparation of thin sections used in the modal analyses. This kind of sample selection was done in order to minimize the effect of inhomogeneity in the rock sample and the effect of difference in size of the system on modal analysis (500 cm^3 sample for PGNAA *versus* thin-section size for modal analyses).

More than 10,000 points were counted for each thin section, repeated three times in order to obtain better statistics. "Theoretical" whole-rock boron contents were estimated using the modal abundance of tourmaline. In this calculation, three boron cations were assumed in the structural formula, and the amount of boron necessary to produce it was calculated from the constraints of stoichiometry.

Although most samples show evidence of a homogeneous distribution of tourmaline crystals within one thin section, sample H9 showed an inhomogeneous distribution of tourmaline crystals, resulting in a large error of calculated whole-rock boron contents. Sample W28 was inappropriate for a determination of the modal compositions by observation of a single thin section because of its very inhomogeneous distribution of tourmaline crystals. Three thin sections of sample W28 were examined, and one contained abundant tourmaline crystals, whereas others did not. In Figure 6, therefore, the value calculated from the sum of the modal analyses of the three thin sections is shown.

DISCUSSION

Reservoir of boron in the upper-amphibolite-facies pelitic–psammitic schists

As is clear from Figure 6, the whole-rock boron contents calculated from the modal proportion of tourma-

line and the whole-rock boron contents determined by PGNAA are in good agreement, showing that the boron in the pelitic–psammitic rocks is almost completely contained in tourmaline. Tourmaline thus is the most important sink of boron in the upper-amphibolite-facies pelitic–psammitic rocks of the Aoyama area.

The presence of the breakdown texture of tourmaline to sillimanite and cordierite near the tourmaline-out isograd and the common occurrence of a sillimanite–cordierite intergrowth in the tourmaline-free region suggest that the tourmaline-out isograd represents the breakdown front of tourmaline (Kawakami 2001). Therefore, an observed drastic drop of the whole-rock boron contents across the tourmaline-out isograd is attributed to the breakdown of tourmaline in the tourmaline-free region.

It is known that sillimanite contains up to 1300 ppm boron in some granulites (Grew & Hinthorne 1983). Pelitic–psammitic migmatites to the south of the tourmaline-out isograd contain up to several modal percent sillimanite, but the low whole-rock boron contents of the sillimanite-bearing migmatite samples imply that sillimanite is not an important sink of boron in the Aoyama area.

Retrograde muscovite is another potential carrier of boron in the migmatite zone. However, low whole-rock boron contents observed throughout the migmatite zone suggest that the formation of retrograde muscovite was not capable of preventing boron from escaping out of the migmatite zone.

Crystal chemistry of tourmaline (*inclusion-poor type of tourmaline*)

Almost all compositions of tourmaline in the pelitic–psammitic rocks from the Aoyama area (exclusive of tourmaline in pegmatite veins) plot in the field of "medium-grade metapelites" or "high-grade metapelites" of Henry & Dutrow (1996) (Fig. 3a). In general, the $Al_2Mg_{-1}Si_{-1}$ exchange becomes more important and the $^{X}\square AlNa_{-1}Mg_{-1}$ exchange becomes less significant in high-grade metamorphic rocks (Henry & Dutrow 1996). The data in Figure 3b suggest that the $Al_2Mg_{-1}Si_{-1}$ exchange is still important in the Aoyama area, as suggested by the weak correlation of Al and Si (Fig. 3c). Figures 3d and 3e suggest that $^{X}\square AlNa_{-1}Mg_{-1}$ and $AlOMg_{-1}(OH)_{-1}$ exchanges are also important, but the almost constant Na value *versus* Al shows that $^{X}\square AlNa_{-1}Mg_{-1}$ is not important in the inclusion-poor type of tourmaline of the Aoyama area.

This result somewhat differs from the experimental results of von Goerne *et al*. (1999), who reported changes in tourmaline composition according to the substitution $^{X}\square AlNa_{-1}Mg_{-1}$ and $AlOMg_{-1}(OH)_{-1}$ as temperature approaches the breakdown temperature of tourmaline in the system Na_2O–MgO–Al_2O_3–SiO_2–B_2O_3–H_2O–HCl. This difference may partly be due to the complexity introduced by Ca in the natural system. As Ca also occupies the *X* site, the proportion of the *X*-site vacancy is also controlled by the substitution involving Ca.

From Figures 3f and 3g, Ca is negatively correlated with Na and ^{Y}Al. A clear correlation between total Al and Ca is not observed. Together with the observation that Mg is negatively correlated with ^{Y}Al, the incorporation of Ca into tourmaline seems controlled by the substitution $CaMgNa_{-1}{}^{Y}Al_{-1}$. Incorporation of Ca should also be controlled by the substitution involving the *X*-site vacancy, since $^{X}\square AlNa_{-1}Mg_{-1}$ has been shown not to be important in the Aoyama area. Figures 3g and 3h imply that the substitution $CaMg_2{}^{X}\square_{-1}{}^{Y}Al_{-2}$ or $CaMgO^{X}\square_{-1}{}^{Y}Al_{-1}(OH)_{-1}$ (Henry & Dutrow 1990b) is operating in the tourmaline of the Aoyama area and controlling the amount of the X-site vacancy.

Incorporation of Ca and the change of the *X*-site vacancy in calcic tourmaline through the substitution $CaMg_2{}^{X}\square_{-1}{}^{Y}Al_{-2}$ was experimentally observed by von Goerne & Frantz (2000), who found that the occupancy of the *X* site by Ca and the amount of Mg increase as temperature increases from 500 to 700°C. Unfortunately, such a clear trend with the change of temperature is difficult to observe in the Aoyama area, partly because of the narrow range of temperature observed (about 100°C). However, if we interpret the tourmaline with a breakdown texture as representing crystals that experienced the highest temperature, and other inclusion-poor-type of crystals to represent tourmaline at lower temperature, there seems to be a trend that Ca and Mg decrease as Al increases at the *Y* site. This is the exact opposite to the trend observed by von Goerne & Frantz (2000) in their experimental study. Further information from the field study will be needed to solve this problem.

Crystal chemistry of tourmaline (*inclusion-rich type of tourmaline*)

Compositions of the core, mantle and rim parts of the inclusion-rich type of tourmaline are plotted as in Figure 3, and exchange vectors that control its chemical variation are determined. A negative correlation between Si and Al, and between Mg and Al, is observed. This may correspond to the $Al_2Mg_{-1}Si_{-1}$ and $AlOMg_{-1}(OH)_{-1}$ exchange vectors. Variation in the *X*-site vacancy may be controlled by the incorporation of Na, since a negative correlation between Na and the proportion of *X*-site vacancy is observed, whereas a correlation between Ca and the proportion of *X*-site vacancy is not observed. A negative correlation between Na and Al suggests that the exchange vector $^{X}\square AlNa_{-1}Mg_{-1}$ is important.

As the proportion of Ca and the *X*-site vacancy does not seem to be correlated, the incorporation of Ca is not controlled by the $CaMg_2{}^{X}\square_{-1}{}^{Y}Al_{-2}$ or $CaMgO^{X}\square_{-1}{}^{Y}Al_{-1}(OH)_{-1}$ exchange vectors, as was the case in the inclusion-poor type of tourmaline. Instead, a clear

negative correlation between Ca and Na may imply that $CaONa_{-1}(OH)_{-1}$ is important here. A positive correlation between Ca and Al is also observed, possibly due to the combination of $CaONa_{-1}(OH)_{-1}$ and $^{X}\square AlNa_{-1}Mg_{-1}$ exchange vectors.

P–T path of the Aoyama area

In the garnet–cordierite zone of the Aoyama area, biotite, sillimanite, cordierite and garnet coexist, and sillimanite is commonly included in cordierite. This association suggests that the reaction

$$Bt + Sil + Qtz = Grt + Crd + Kfs \pm Ilm + melt \quad (2)$$

took place (Kawakami 2001). Because reaction (2) is the most important to ensure a marked increase in the fraction of melt in pelitic–psammitic rocks (*e.g.*, White *et al*. 2001), it is apparent that migmatite formation in the garnet–cordierite zone of the Aoyama area is largely due to this reaction. The P–T location of reaction (2) is shown in Figure 7. Although the P–T grid of the suprasolidus part of the Figure 7 is based on a P–T pseudosection for the bulk composition of average metapelite (Powell *et al*. 1998), as calculated in White *et al*. (2001), at least P–T locations of reaction (2) and the reaction

$$Bt + Sil + Qtz = Crd + Kfs + melt \quad (3)$$

are similar to the P–T grid of Brown (1998) calculated for the bulk composition of Ryoke metamorphic rocks. Therefore, usage of Figure 7 in constructing the P–T paths of the Aoyama area should not cause large discrepancies. In Figure 7, path A is representative of the P–T evolution of the sillimanite – K-feldspar zone, path B is representative of the low-temperature part of the garnet–cordierite zone, and path C pertains to the high-temperature part of the garnet–cordierite zone.

The P–T location of reaction (2) will be shifted to the low-temperature side if Mn is present in the system, because Mn preferentially enters into garnet and stabilizes it (*e.g.*, Mahar *et al*. 1997). This effect probably was more important in the low-temperature part of the garnet–cordierite zone than at higher temperature in that zone because garnet coexisting with cordierite in the low-temperature part shows higher Mn contents (up to 8.5 wt% MnO in the rim of the garnet in sample L4, whereas the rim of the garnet in sample Y49b, which belongs to the high-temperature part of the garnet–cordierite zone, contains 3.5 wt% MnO). It is possible, therefore, that coexistence of garnet and cordierite in the low-temperature part of the garnet–cordierite zone is due to the effect of Mn. Therefore, the peak P–T conditions of this region are considered to be on the low-temperature side of the reaction (2) in the system KFMASH (path B in Fig. 7).

Another important reaction that will contribute to the drastic increase of the melt fraction is the dehydration melting of muscovite (*e.g.*, Vielzeuf & Holloway 1988, White *et al*. 2001). The invariant point defined by the intersection between the muscovite-dehydration reaction and the wet haplogranite solidus [point I for $a(H_2O) = 0.8$ in Fig. 7] is located near the boundary of the sillimanite – K-feldspar zone and the garnet–cordierite zone in the P–T space where $a(H_2O)$ is high. The possibility should be considered, therefore, that a melting reaction involving muscovite played an important role in the formation of migmatites in the Aoyama area.

The pelitic–psammitic rocks of the Aoyama area ubiquitously contain plagioclase and quartz and, therefore, the muscovite-consuming reaction may well have contained albite as a reactant. In the sillimanite – K-feldspar zone, the migmatite texture is rare, and evidence for the occurrence of partial melting, such as crystal faces of K-feldspar against quartz or euhedral plagioclase (*e.g.*, Vernon & Collins 1988, Tagiri *et al*. 1995) is only locally found (Kawakami 2001). This observation may imply that the dehydration-melting reaction

$$Ms + Ab + Qtz = Kfs + Sil + melt \quad (4)$$

did not take place in the sillimanite – K-feldspar zone, even at the peak temperature. The local occurrence of euhedral plagioclase in the sillimanite – K-feldspar zone may be due to the vapor-present melting that took place locally at the peak temperature in the high $a(H_2O)$ part of the rock. The common absence of muscovite, the presence of the sillimanite + K-feldspar assemblage, and the non-anatectic nature of the pelitic–psammitic rocks in the sillimanite – K-feldspar zone suggest that subsolidus breakdown of muscovite occurred through the reaction

$$Ms + Ab + Qtz = Kfs + Als + vapor \quad (5)$$

Muscovite will be consumed by this reaction because pelitic–psammitic rocks commonly contain more plagioclase and quartz than muscovite, and the rocks remain unmelted. Reaction (5) should, therefore, be located at the low-temperature side of the P–T conditions of the sillimanite – K-feldspar zone. The ubiquitous existence of graphite in the pelitic–psammitic schists and migmatites suggests that $a(H_2O)$ is less than 1.0, and CO_2 and CH_4 must have been present with H_2O in the fluid (Ohmoto & Kerrick 1977). In order to fulfill these restrictions, $a(H_2O) < 0.8$ is required (Fig. 7). The textural study of Kawakami (2001) suggests that the prograde P–T path of the sillimanite – K-feldspar zone should cross reaction (5) first, and then the andalusite–sillimanite reaction to reach peak P–T conditions (path A in Fig. 7).

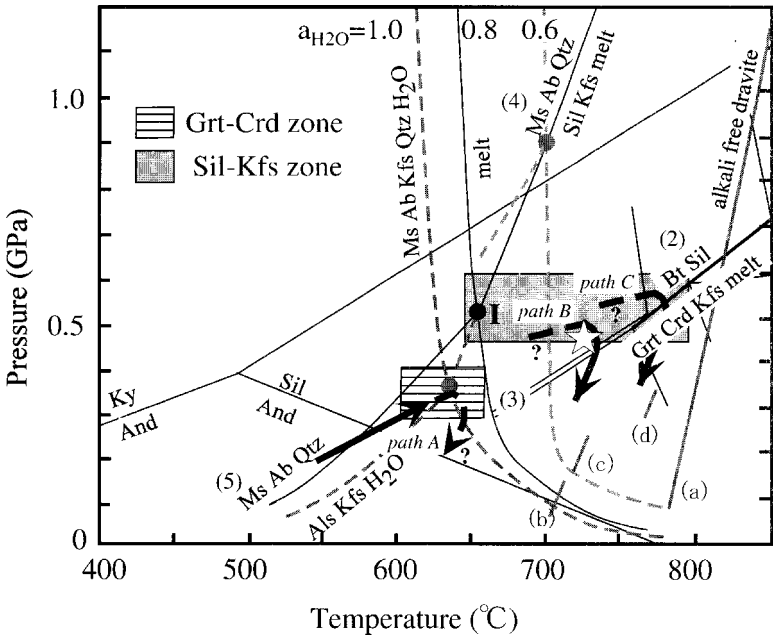

FIG. 7. P–T diagram showing the peak conditions attained in the sillimanite–cordierite and garnet–cordierite zones and the provisional location of the breakdown reaction of tourmaline in the Aoyama area (white star). The melting curves involving muscovite, quartz, K-feldspar, aluminosilicate, albite and H_2O are taken from Johannes & Holtz (1996). Some reaction curves are omitted for simplicity. The solid black lines represent the reaction curves for $a(H_2O)$ = 0.8, and the dashed lines represent those for $a(H_2O)$ values of 0.6 and 1.0. Solid black lines shown in the suprasolidus region are the P–T pseudosection in the KFMASH system (White *et al*. 2001) constructed for the bulk composition of an average pelite (Powell *et al*. 1998). Important reactions are Bt + Sil + Qtz = Grt + Crd + Kfs + melt [reaction (2)] and Bt +Sil + Qtz = Crd + Kfs + melt [reaction (3)], P–T locations of which are nearly the same as in Figure 8 of Brown (1998). Solid gray lines in the suprasolidus region are the selected experimental results of the high-temperature stability limit of tourmaline: (a) alkali-free dravite + boron-rich fluid (Werding & Schreyer 1984), (b) alkali-free dravite without excess boron in the fluid (Werding & Schreyer 1984), (c) dravite + quartz with more than 4 wt% B_2O_3 in the final fluid (von Goerne *et al*. 1999), (d) natural schorl + gneiss (Holtz & Johannes 1991). The aluminosilicate phase diagram conforms to that of Holdaway (1971). The P–T paths (thick arrows) for the sillimanite – K-feldspar and garnet–cordierite zones are estimated from the petrographic observations in Kawakami (2001). The numbers of the reaction (2)–(5) are identical to those used in the text. Modified from Kawakami (2001).

It is difficult to determine whether muscovite decomposed through the subsolidus dehydration reaction or the dehydration-melting reaction in the garnet–cordierite zone, which is greatly controlled by the $a(H_2O)$ in the pelitic–psammitic rocks. If the P–T grid of muscovite-consuming reactions for $a(H_2O)$ = 0.8 is adopted, it is possible for rocks in the high-temperature part of the garnet–cordierite zone to cross-cut the muscovite dehydration-melting curve, provided that the prograde P–T path involved nearly isobaric heating. In case of $a(H_2O)$ < 0.8, muscovite will be consumed through the subsolidus breakdown-reaction (5).

Because muscovite is an important carrier of boron in medium-grade metasediments (*e.g.*, Henry & Dutrow 1996), the stability of muscovite is important in considering the behavior of boron in the pelitic–psammitic rocks, which will be discussed below.

P–T location of the tourmaline-breakdown reaction

The provisional P–T location of the tourmaline-out isograd has been estimated as a point of intersection between the metamorphic field-gradient of the Aoyama area and the P–T conditions of low-temperature part of

the garnet–cordierite zone (Kawakami 2001). The P–T estimates are mainly based on the result of geothermometry and geobarometry, in light of estimates of the relevant closure temperature. Further consideration of the P–T conditions in this study on the basis of P–T grids show that the highest-grade rocks in the garnet–cordierite zone may have been metamorphosed at a higher temperature than previously estimated. This implies that the metamorphic field-gradient had a shallower slope (*i.e.*, smaller dP/dT), and thus the provisional location of the tourmaline-out isograd is shifted to a higher temperature than Kawakami (2001) had proposed, to about 725°C, 4.5 kbar.

Although there are many high-temperature experiments dealing with the stability limit of tourmaline, they are mostly limited to low pressures, around 2–3 kbar (Benard *et al*. 1985, Morgan & London 1989, Holtz & Johannes 1991, von Goerne *et al*. 1999, 2001, von Goerne & Frantz 2000). The limited range of pressure among these experimental studies makes it difficult to evaluate the effect of pressure on the breakdown temperature of tourmaline in complex model systems. Schreyer & Werding (1997) reported that at a pressure of 5 kbar, dravite + boron-rich fluid breaks down at 900°C, whereas alkali-free dravite breaks down at 830°C in the presence of boron-rich fluid [(a) in Fig. 7]. These results suggest that the increase of the *X*-site vacancy in tourmaline may reduce the stability field of tourmaline at constant pressures. Werding & Schreyer (1984) reported that the high-temperature limit of stability of alkali-free dravite without excess boron is observed at 730°C, 1 kbar [(b) in Fig. 7]. Low boron contents in the fluid thus may also lower the breakdown temperature of tourmaline.

The breakdown temperature of tourmaline inferred from the field study is a little lower than that estimated from the laboratory experiments. The difference may mainly result from the different breakdown-reaction of tourmaline in the natural environment caused by the addition of other minerals as reactants. It is also likely that the difference in the composition of tourmaline, especially the amount of the *X*-site vacancy, and of the fluid phase, exerts a control on the temperature of breakdown.

Different behavior of boron in the tourmaline-present and tourmaline-absent regions

The existence of tourmaline in the tourmaline-present region (mostly belonging to the sillimanite – K-feldspar zone and the low-temperature part of the garnet–cordierite zone) implies that the P–T path of this region did not reach the breakdown reaction of tourmaline (path A). In this region, breakdown of muscovite may have occurred by subsolidus dehydration according to reaction (5) and the boron-bearing fluid released may have contributed to the overgrowths of tourmaline (Henry & Dutrow 1990a). The rim part of the inclusion-poor type of tourmaline may represent the breakdown product of muscovite.

On the other hand, the tourmaline-absent region (mostly belonging to the high-temperature part of the garnet–cordierite zone) suggests that the P–T path of this region did cross the breakdown reaction of tourmaline at around 730°C (path C).

The behavior of boron before reaching the breakdown of tourmaline may differ, depending on the mode of breakdown reaction of muscovite. If the breakdown of muscovite in this region occurred by the dehydration melting reaction (4), boron-bearing melt will be formed without the formation of the overgrowth of tourmaline. Boron contained in the muscovite should be mostly incorporated in the melt because of its incompatible nature. Boron released by the subsequent breakdown of tourmaline may also be incorporated in the melt. If the breakdown of muscovite occurred by subsolidus reaction (5), the boron released will form the overgrowth on tourmaline as in the case of the tourmaline-present region described herein. As suggested by the absence of tourmaline, further increase in temperature should lead to a crossing of the breakdown reaction of tourmaline, and boron will be incorporated in the melt also in this case.

By which reaction muscovite breaks down is controlled by the prograde P–T path in the tourmaline-absent region (shown with "?" in paths B and C) and $a(H_2O)$ at the site of muscovite breakdown. Although breakdown of muscovite through the subsolidus dehydration reaction is likely, further study is needed to solve this problem.

The expected difference in the behavior of boron between the tourmaline-present region, in which subsolidus breakdown of muscovite enabled the overgrowth of tourmaline, and the tourmaline-absent region, in which breakdown of tourmaline enabled boron to be incorporated in the melt, may be one important reason for the sharpness of the tourmaline-out isograd.

Mechanism for the extraction of boron from the migmatite zone

The depletion of boron in the migmatite zone may be potentially related to the formation of tourmaline leucogranites *via* the migration of boron-bearing melts. This is because the P–T conditions estimated for the formation of tourmaline leucogranites is similar to those estimated for the migmatite zone (*e.g.*, Le Fort 1981, Murata 1984, Le Fort *et al*. 1987, Nabelek *et al*. 1992, Barbey *et al*. 1996). Nabelek *et al*. (1992) suggested that small degree of dehydration melting of muscovite is important for the formation of the Harney Peak leucogranite, without a need for the breakdown of boron-rich phases. If muscovite breaks down to produce boron-bearing melt in the source region of the tourmaline leucogranites, boron contained in muscovite will not contribute on the growth of tourmaline and thus the

breakdown of tourmaline may be less important. However, if muscovite breaks down by the subsolidus dehydration-reaction, boron contained in the muscovite may contribute on the overgrowth of tourmaline (*e.g.*, Henry & Dutrow 1990a) and thus consideration on the breakdown of tourmaline will become significant in modeling the behavior of boron.

The very low whole-rock boron contents observed throughout the migmatite zone of the Aoyama area (Fig. 4, Table 2) implies that boron was effectively removed from the migmatite zone through the movement of melts or fluids (or both). Thomas *et al*. (2000) studied the melt inclusions in pegmatite quartz and found that the presence of high concentrations of fluorine, boron and phosphorus dramatically reduces the critical pressure for fluid–melt systems. Complete miscibility between fluid and melt is shown to exist above 712°C at about 1 kbar (Thomas *et al*. 2000). Considering the temperature attained in the Aoyama area (Fig. 7), it is possible that boron was extracted from the migmatite zone by the movement of a supercritical fluid. Although it is difficult to identify the exact mechanism that took place in the Aoyama area, possible cases are discussed below.

Because of the similarity of whole-rock compositions of the pelitic–psammitic schists and migmatites in terms of major elements (Fig. 5), a significant amount of extraction of melt or supercritical fluid from the migmatite zone does not seem to be plausible. Extraction of boron from the migmatite zone may, therefore, be limited to the extraction of small amounts of boron-bearing melt, aqueous fluid or supercritical fluid. Field evidence for this process, such as the presence of tourmaline-bearing leucogranite sills (*e.g.*, Le Fort *et al*. 1987, Johannes & Holtz 1996) is, however, not present in the Aoyama area except for the tourmaline-bearing pegmatite veins.

The extraction of boron in the melt (or supercritical fluid) is possible mainly in two stages. The first one is in the prograde stage, in the case that the breakdown of tourmaline occurred at a relatively early stage with a low degree of melting. Under such circumstances, boron-bearing melt formed by the breakdown of tourmaline may segregate as soon as it is formed because of its buoyancy and low viscosity. The amount of the melt formed will be small, as suggested by the low modal proportion of tourmaline. Therefore, segregation of the boron-bearing melt does not cause a drastic change to the whole-rock compositions. This case would correspond to fractional melting.

The second case is expected at the retrograde stage. Extraction of small amount of boron-bearing melt (or supercritical fluid) may be possible through fractional crystallization of the leucosome melts, which may contribute to the formation of evolved, boron- and vapor-rich melts of low viscosity.

The extraction of aqueous fluids also is important, especially in the case of the elements that are strongly partitioned into the aqueous fluid relative to the coexisting melt. Boron has a low to medium partition-coefficient between the melt and the aqueous fluid, $K_d(B_2O_3)$(melt/fluid) being 0.33 (Pichavant 1981) or 0.43–1.0 (London *et al.* 1988). Extraction of boron in the aqueous fluid is consistent with the similarity of whole-rock chemistry in terms of major elements between schists and migmatites.

In order for the extraction of boron to occur *via* the extraction of a boron-bearing aqueous fluid, the attainment of H_2O saturation should occur before tourmaline starts to crystallize from the leucosome melts in the migmatite. Although the melt may be undersaturated in H_2O upon its formation, saturation of the melt in H_2O may be attained through segregation and fractional crystallization of the melt, which results in the small extent of back reactions in the migmatite zone. Such a small extent is suggested by the well-preserved residual phases such as garnet and cordierite. Saturation in H_2O can also be attained through decompression of the area because the solubility of H_2O in the silicate melts decreases with decreasing pressure (*e.g.*, Johannes & Holtz 1996).

Another possible way to extract boron *via* the extraction of fluid or "fluid-rich melt" (Thomas *et al*. 2000) is to consider the extent of immiscibility in the system. If the solvus for the supercritical fluid is crossed in the migmatite zone upon cooling, then boron will be strongly partitioned into the "fluid-rich melt" rather than into the "silicate-rich melt" (Thomas *et al*. 2000). Such a melt may have a lower viscosity and density than the "silicate-rich melt" and thus may have been easy to extract from the migmatite zone.

Where did the boron go? A mass-balance problem

The tourmaline-bearing pegmatite veins found in the north of the tourmaline-out isograd (Fig. 2) are potential candidates to account for the melt or fluid extracted from the migmatite zone. Assuming that pegmatite veins of 1 m width containing 100 tourmaline crystals (10^2 cm^3 each) per 1 m^3 occur every 10 m, and that 0.1 vol.% tourmaline was previously contained in the protolith of the migmatites, a mass-balance calculation suggests that the concentration of boron in one tourmaline-bearing pegmatite vein can account for the boron depletion in the migmatite zone of the same length. That is, pegmatite veins with length of 1 km can account for boron-depletion zone 1–2 km wide in the migmatite zone. Therefore, tourmaline-bearing pegmatite veins are significant as one possible sink of boron extracted from the migmatite-zone, but are not abundant enough to explain all the boron that may have been originally present in the protoliths of the migmatites.

It is possible that evidence for extracted boron-bearing melts or fluids has been partly lost by erosion. However, in a search for the sink of boron in the field, tourmaline crystals that occur on the low-grade side of

the tourmaline-out isograd may be potentially important. If a percolation flow of boron-bearing melt or fluid originating from the migmatite zone took place as well as localized channel-flows, it may have brought about the retrograde growth of tourmaline in the tourmaline-stable region. In this case, tourmaline crystals that occur in the low-grade side of the tourmaline-out isograd should be regarded as the sum of the crystals that survived the prograde metamorphism and any newly precipitated crystals from the percolating melt or fluid. Evidence for the occurrence of such percolation flow is, however, presently not observed, and apparently retrograde tourmaline is found exclusively in veins.

It is known that terrestrial sediments generally contain about 100 ppm boron (London *et al.* 1996). In addition, preliminary data of boron contents in one sample of pelitic rock from the Mino–Tanba belt showed 112 ppm (Table 2). If this value (112 ppm) is taken as representative of the primary boron contents of the protoliths of pelitic–psammitic metamorphic rocks in the Aoyama area, it follows that more than 20% of the whole-rock boron has been lost through dehydration reactions of illite or muscovite in the sillimanite – K-feldspar zone rocks. This view is partly consistent with that of previous workers who ascribed the progressive depletion of boron by the regional metamorphism to dehydration reactions involving illite or muscovite (Shaw *et al.* 1988, Leeman *et al.* 1992, Moran *et al.* 1992, Bebout *et al.* 1993). In the tourmaline-bearing rocks, however, at most 80% of whole-rock boron remains in tourmaline, pointing to the importance of tourmaline in modeling the behavior of boron.

Conclusions

1. A petrological and geochemical study has shown that tourmaline is the most important sink of boron in pelitic–psammitic rocks recrystallized to the upper-amphibolite facies, and that its stability almost completely controls the behavior of whole-rock boron in the Aoyama area, Ryoke metamorphic belt, southwestern Japan.

2. The $^{X}\square AlNa_{-1}Mg_{-1}$ exchange is insignificant, but the $Al_2Mg_{-1}Si_{-1}$, $AlOMg_{-1}(OH)_{-1}$ and $CaMg_2{}^{X}\square_{-1}{}^{Y}Al_{-2}$ or $CaMgO^{X}\square_{-1}{}^{Y}Al_{-1}(OH)_{-1}$ exchanges are important in tourmaline at the P–T conditions of its breakdown. The amount of the *X*-site vacancy is controlled by the incorporation of Ca into tourmaline in the Aoyama area.

3. The behavior of boron is modeled on the basis of the P–T evolution of the Aoyama area, especially concentrating on the stability of muscovite and tourmaline.

4. The breakdown of tourmaline and the subsequent extraction of small amounts of boron-bearing melt, aqueous fluid or supercritical fluid from the migmatite zone upon the crystallization of leucosome melt may be responsible to the depletion of boron in the migmatites. Tourmaline-bearing pegmatite veins observed on the northern side of the tourmaline-out isograd are one of the candidates for the sinks of boron extracted from the migmatite zone.

Acknowledgements

I am grateful to M. Obata and T. Hirajima for discussion and improvements to the manuscript. I thank R. Tsurudome for the support in XRF analyses, D.M. Shaw and M.D. Pereira for advice and information on PGNAA for boron in neutron-activation analsys at McMaster University, and H. Tsutsumi and K. Yoshida for preparation of thin sections. I thank two anonymous referees for their constructive reviews of the manuscript, and R.F. Martin for careful editorial assistance. This study was supported financially by the JSPS Research Fellowship for Young Scientists.

References

Acosta, A., Pereira, M.D. & Shaw, D.M. (2000): Influence of volatiles in the generation of crustal anatectic melts. *J. Geochem. Explor.* **69-70**, 339-342.

_____, _____, Shaw, D.M. & London, D. (2001): Contrasting behavior of boron during crustal anatexis. *Lithos* **56**, 15-31.

Barbey, P., Brouand, M., Le Fort, P. & Pecher, A. (1996): Granite–migmatite genetic link: the example of the Manaslu granite and Tibetan Slab migmatites in central Nepal. *Lithos* **38**, 63-79.

Bebout, G.E., Ryan, J.G. & Leeman, W.P. (1993): B–Be systematics in subduction-related metamorphic rocks. Characterization of the subducted component. *Geochim. Cosmochim. Acta* **57**, 2227-2237.

Benard, F., Moutou, P. & Pichavant, M. (1985): Phase relations of tourmaline leucogranites and the significance of tourmaline in silicic magmas. *J. Geol.* **93**, 271-291.

Brown, M. (1973): The definition of metatexis, diatexis and migmatite. *Proc. Geologists' Assoc.* **84**, 371-382.

_____ (1998): Unpairing metamorphic belts: P–T paths and a tectonic model for the Ryoke Belt, southwest Japan. *J. Metamorph. Geol.* **16**, 3-22.

_____, Averkin, Y.A. & McLellan, E.L. (1995): Melt segregation in migmatites. *J. Geophys. Res.* **100**, 15655-15679.

_____ & Rushmer, T. (1997): The role of deformation in the movement of granitic melt: views from the laboratory and the field. *In* Deformation-Enhanced Fluid Transportation in the Earth's Crust and Mantle (M.B. Holness, ed.). Chapman & Hall, London, U.K. (110-144).

Dingwell, D.B., Knoche, R., Webb, S.L., & Pichavant, M. (1992): The effect of B_2O_3 on the viscosity of haplogranitic liquids. *Am. Mineral.* **77**, 457-461.

DUTROW, B.L., FOSTER, C.T., JR. & HENRY, D.J. (1999): Tourmaline-rich pseudomorphs in sillimanite zone metapelites: demarcation of an infiltration front. *Am. Mineral.* **84**, 794-805.

GOTO, A. & TATSUMI, Y. (1994): Quantitative analysis of rock samples by an X-ray fluorescence spectrometer (I). *The Rigaku Journal* **11**, 40-59.

GREW, E.S. & HINTHORNE, J.R. (1983): Boron in sillimanite. *Science* **221**, 547-549.

HAWTHORNE, F.C. (1996): Structural mechanisms for light-element variations in tourmaline. *Can. Mineral.* **34**, 123-132.

_____ & HENRY, D.J. (1999): Classification of the minerals of the tourmaline group. *Eur. J. Mineral.* **11**, 201-215.

HAYAMA, Y., YAMADA, T., ITO, M., KUTSUKAKE, T., MASAOKA, K., MIYAKAWA, K., MOCHIZUKI, Y., NAKAI, Y., TAINOSHO, Y., YOSHIDA, M., KAWARABAYASHI, I. & TSUMURA, Y. (1982): Geology of the Ryoke Belt in the eastern Kinki District, Japan – the phase-divisions and the mutual relations of the granitic rocks. *J. Geol. Soc. Japan* **88**, 451-466.

HENRY, D.J. & DUTROW, B.L. (1990a): Evolution of tourmaline in metapelitic rocks; diagenesis to melting. *Geol. Soc. Am., Abstr. Programs* **22**, 125.

_____ & _____ (1990b): Ca substitution in Li-poor aluminous tourmaline. *Can. Mineral.* **28**, 111-124.

_____ & _____ (1996): Metamorphic tourmaline and its petrologic applications. *In* Boron: Mineralogy, Petrology and Geochemistry (E.S. Grew & L.M. Anovitz, eds.). *Rev. Mineral.* **33**, 503-557.

_____ & GUIDOTTI, C.V. (1985): Tourmaline as a petrogenetic indicator mineral: an example from the staurolite-grade metapelites of NW Maine. *Am. Mineral.* **70**, 1-15.

HIGASHIMOTO, S., NUREKI, T., HARA, I., TSUKUDA, E. & NAKAJIMA, T. (1983): Geology of the Iwakuni district. *Geol. Surv. Japan, Quadrangle Ser.* (scale 1: 50,000).

HIGGINS, M.D., TRUSCOTT, M.G., SHAW, D.M., BERGERON, M., BUFFET, G.H., COPLEY, J.R.D. & PRESTWICK, W.V. (1984): Prompt-gamma neutron activation analysis at McMaster nuclear reactor. *Atomkern-energie Kerntechnik* **44**, 690-697.

HIRAJIMA, T. & BANNO, S. (1991): Electron-microprobe analysis of rock-forming minerals with Kevex-Delta IV Quantum Detector. *Hitachi Scientific Instrument News* **34**, 2-7 (in Japanese).

HOLDAWAY, M.J. (1971): Stability of andalusite and the aluminum silicate phase diagram. *Am. J. Sci.* **271**, 97-131.

HOLTZ, F. & JOHANNES, W. (1991): Effect of tourmaline on melt fraction and composition of first melts in quartzo-feldspathic gneiss. *Eur. J. Mineral.* **3**, 527-536.

IKEDA, T. (1993): Compositional zoning patterns of garnet during prograde metamorphism from the Yanai district, Ryoke metamorphic belt, southwest Japan. *Lithos* **30**, 109-121.

_____ (1998a): Progressive sequence of reactions of the Ryoke metamorphism in the Yanai district, southwest Japan: the formation of cordierite. *J. Metamorph. Geol.* **16**, 39-52.

_____ (1998b): Phase equilibria and the pressure–temperature path of the highest-grade Ryoke metamorphic rocks in the Yanai district, SW Japan. *Contrib. Mineral. Petrol.* **132**, 321-335.

JOHANNES, W. & HOLTZ, F. (1996): *Petrogenesis and Experimental Petrology of Granitic Rocks*, Springer-Verlag, Berlin, Germany.

KAWAKAMI, T. (2000): Tourmaline breakdown and boron depletion in the migmatite-zone of the Ryoke metamorphic belt, Japan. *Eos, Trans. Am. Geophys. Union* **81**, 236 (abstr.).

_____ (2001): Tourmaline breakdown in the migmatite zone of the Ryoke metamorphic belt, SW Japan. *J. Metamorph. Geol.* **19**, 61-75.

KRETZ, R. (1983): Symbols for rock forming minerals. *Am. Mineral.* **68**, 277-279.

LEEMAN, W.P., SISSON, V.B. & REID, M.R. (1992): Boron geochemistry of the lower crust: evidence from granulite terranes and deep crustal xenoliths. *Geochim. Cosmochim. Acta* **56**, 775-788.

LE FORT, P. (1981): Manaslu leucogranite: a collision signature of the Himalaya. A model for its genesis and emplacement. *J. Geophys. Res.* **86**, 10545-10568.

_____ , CUNEY, M., DENIEL, C., FRANCE-LANORD, C., SHEPPARD, S.M.F., UPRETI, B.N. & VIDAL, P. (1987): Crustal generation of the Himalayan leucogranites. *Tectonophys.* **134**, 39-57.

LONDON, D., HERVIG, R.L. & MORGAN, G.B., VI (1988): Melt–vapor solubilities and elemental partitioning in peraluminous granite–pegmatite systems: experimental results with Macusani glass at 200 MPa. *Contrib. Mineral. Petrol.* **99**, 360-373.

_____ , MORGAN, G.B. VI & WOLF, M.B. (1996): Boron in granitic rocks and their contact aureoles. *In* Boron: Mineralogy, Petrology and Geochemistry (E.S. Grew & L.M. Anovitz, eds.). *Rev. Mineral.* **33**, 299-330.

MAHAR, E.M., BAKER, J.M., POWELL, R., HOLLAND, T.J.B. & HOWELL, N. (1997): The effect of Mn on mineral stability in metapelites. *J. Metamorph. Geol.* **15**, 223-238.

MIYASHIRO, A. (1965): *Metamorphic Rocks and Metamorphic Belts*. Iwanami Shoten, Tokyo, Japan (in Japanese).

_____ (1994): *Metamorphic Petrology*. UCL Press Ltd, London, U.K.

MORAN, A.E., SISSON, V.B. & LEEMAN, W.P. (1992): Boron depletion during progressive metamorphism: implications for subduction processes. *Earth Planet. Sci. Lett.* **111**, 331-349.

MORGAN, G.B. & LONDON, D.(1989): Experimental reactions of amphibolite with boron-bearing aqueous fluids at 200 MPa: implications for tourmaline stability and partial melting in mafic rocks. *Contrib. Mineral. Petrol.* **102**, 281-297.

MORI, T. & KANEHIRA, K. (1984): X-ray energy spectrometry for electron-probe analysis. *J. Geol. Soc. Japan* **90**, 271-285.

MURATA, M. (1984): Petrology of Miocene I-type and S-type granitic rocks in the Ohmine district, central Kii peninsula. *J. Japan. Assoc. Mineral. Petrol. Econ. Geol.* **79**, 351-369.

NABELEK, P.I., RUSS-NABELEK, C. & DENISON, J.R. (1992): The generation and crystallization conditions of the Proterozoic Harney Peak leucogranite, Black Hills, South Dakota, USA: petrologic and geochemical constraints. *Contrib. Mineral. Petrol.* **110**, 173-191.

NAKAJIMA, T. (1994): The Ryoke plutonometamorphic belt: crustal section of the Cretaceous Eurasian continental margin. *Lithos* **33**, 51-66.

_____, SHIRAHASE, T. & SHIBATA, K. (1990): Along-arc lateral variation of Rb–Sr and K–Ar ages of Cretaceous granitic rocks in southwest Japan. *Contrib. Mineral. Petrol.* **104**, 381-389.

OHMOTO, H. & KERRICK, D.M. (1977): Devolatilization equilibria in graphitic systems. *Am. J. Sci.* **277**, 1013-1044.

OKUDAIRA, T. (1996): Temperature–time path for the low-pressure Ryoke metamorphism, Japan, based on chemical zoning in garnet. *J. Metamorph. Geol.* **14**, 427-440.

_____, HARA, I., SAKURAI, Y. & HAYASAKA, Y. (1993): Tectono-metamorphic processes of the Ryoke belt in the Iwakuni–Yanai district, southwest Japan. *Geol. Soc. Japan, Mem.* **42**, 91-120.

ONO, A. (1977): Petrologic study of the Ryoke metamorphic rocks in the Takato–Shiojiri area, central Japan. *J. Japan. Assoc. Mineral. Petrol. Econ. Geol.* **72**, 453-468.

PEREIRA, M.D. & SHAW, D.M. (1997): Behaviour of boron in the generation of an anatectic complex: the Peña Negra complex, central Spain. *Lithos* **40**, 179-188.

PICHAVANT, M. (1981): An experimental study of the effect of boron on a water saturated haplogranite at 1 kbar vapour pressure. *Contrib. Mineral. Petrol.* **76**, 430-439.

POWELL, R., HOLLAND, T.J.B. & WORLEY, B. (1998): Calculating phase diagrams involving solid solutions via non-linear equations, with examples using THERMOCALC. *J. Metamorph. Geol.* **16**, 577-588.

SAWYER, E.W. (1996): Melt segregation and magma flow in migmatites: implications for the generation of granite magmas. *Trans. R. Soc. Edinburgh: Earth Sci.* **87**, 85-94.

SCHREYER, W. & WERDING, G. (1997): High-pressure behaviour of selected boron minerals and the question of boron distribution between fluids and rocks. *Lithos* **41**, 251-266.

SHAW, D.M. & SMITH, P.L. (1991) Concentrations of B, Sm, Gd, and H in 24 reference materials. *Geostandards Newsletter* **15**, 58-66.

_____, TRUSCOTT, M.G., GRAY, E.A. & MIDDLETON, T.A. (1988): Boron and lithium in high-grade rocks and minerals from the Wawa–Kapuskasing region, Ontario. *Can. J. Earth Sci.* **25**, 1485-1502.

SPERLICH, R., GIERÉ, R. & FREY, M. (1996): Evolution of compositional polarity and zoning in tourmaline during prograde metamorphism of sedimentary rocks in the Swiss Central Alps. *Am. Mineral.* **81**, 1222-1236.

SUZUKI, K. & ADACHI, M. (1998): Denudation history of the high T/P Ryoke metamorphic belt, southwest Japan: constraints from CHIME monazite ages of gneisses and granitoids. *J. Metamorph. Geol.* **16**, 23- 37.

TAGIRI, M., TANAKA, H. & SHIBA, M. (1995): Melting of amphibolites and the form of melt-trap in amphibolite–migmatites of the southern Hidaka metamorphic belt, Hokkaido, Japan. *J. Japan. Assoc. Mineral. Petrol. Econ. Geol.* **90**, 50-63.

TAKAHASHI, Y. & NISHIOKA, Y. (1994): Mode of plagioclase twinnings in Ryoke metamorphic rocks in the western area of Tsu City, Mie Prefecture. *J. Japan. Assoc. Mineral. Petrol. Econ. Geol.* **89**, 261-268.

THOMAS, R., WEBSTER, J.D. & HEINRICH, W. (2000): Melt inclusions in pegmatite quartz: complete miscibility between silicate melts and hydrous fluids at low pressure. *Contrib. Mineral. Petrol.* **139**, 394-401.

VERNON, R.H. & COLLINS, W.J. (1988): Igneous microstructures in migmatites. *Geology* **16**, 1126-1129.

VIELZEUF, D. & HOLLOWAY, J.R. (1988): Experimental determination of the fluid-absent melting relations in the pelitic system. Consequences for the crustal differentiation. *Contrib. Mineral. Petrol.* **98**, 257-276.

VON GOERNE, G. & FRANZ, G. (2000): Synthesis of Ca-tourmaline in the system $CaO–MgO–Al_2O_3–SiO_2–B_2O_3–H_2O–HCl$. *Mineral. Petrol.* **69**, 161-182.

_____, _____ & HEINRICH, W. (2001): Synthesis of tourmaline solid solutions in the system $Na_2O–MgO–Al_2O_3–SiO_2–B_2O_3–H_2O–HCl$ and the distribution of Na between tourmaline and fluid at 300 to 700 and 200 MPa. *Contrib. Mineral. Petrol.* **141**, 160-173.

_____, _____ & ROBERT, J.–L. (1999): Upper thermal stability of tourmaline + quartz in the system $MgO–Al_2O_3–SiO_2–B_2O_3–H_2O$ and $Na_2O–MgO–Al_2O_3–SiO_2–B_2O_3–H_2O–HCl$ in hydrothermal solutions and siliceous melts. *Can. Mineral.* **37**, 1025-1039.

WAKITA, K. (1987): The occurrence of latest Jurassic – earliest Cretaceous radiolarians at the Hida–Kanayama area in the

Mino terrane, central Japan. *J. Geol. Soc. Japan* **93**, 441-443.

WERDING, G. & SCHREYER, W. (1984): Alkali-free tourmaline in the system $MgO–Al_2O_3–B_2O_3–SiO_2–H_2O$. *Geochim. Cosmochim. Acta* **48**, 1331-1344.

WHITE, R.W., POWELL, R. & HOLLAND, T.J.B. (2001): Calculation of partial melting equilibria in the system $Na_2O–CaO–FeO–MgO–Al_2O_3–SiO_2–H_2O$ (NCKFMASH). *J. Metamorph. Geol.* **19**, 139-153.

WILLIAMS, M.L., HANMER, S., KOPF, C. & DARRACH, M. (1995): Syntectonic generation and segregation of tonalitic melts from amphibolite dikes in the lower crust, Striding–Athabasca mylonite zone, northern Saskatchewan. *J. Geophys. Res.* **100**, 15717-15734.

YOSHIDA, F., TAKAHASHI, Y. & NISHIOKA, Y. (1995): Geology of the Tsu–Seibu district. *Geol. Surv. Japan, Map* (1:50,000).

YOSHIZAWA, H., NAKAJIMA, W. & ISHIZAKA, K. (1966): The Ryoke metamorphic zone of the Kinki district, southwest Japan: accomplishment of a regional geological map. *Mem. College of Science, Univ. Kyoto, Ser. B* **32**, 437-453.

Received April 22, 2001, revised manuscript accepted November 12, 2001.